Thickness dependence of the elastic modulus of tris(8-hydroxyquinolinato)aluminium†‡

Jessica M. Torres,[a] Nathan Bakken,[b] Christopher M. Stafford,[c] Jian Li[b] and Bryan D. Vogt[*a]

The intrinsic flexibility of organic molecular films has been suggested to enable bendable electronics in comparison to their stiffer, inorganic counterparts. However, very little is known regarding the mechanical properties of these molecular glasses that are commonly utilized in organic electronics. To begin to address these issues, the elastic modulus of vapor deposited tris(8-hydroxyquinolinato)aluminium (Alq_3) films, commonly used in organic light emitting devices (OLEDs), is determined as a function of thickness from 10 nm to 100 nm using a wrinkling-based metrology. These thicknesses correspond well with the range actually utilized in OLEDs. The direct deposition of Alq_3 onto a polydimethylsiloxane (PDMS) elastomer results in anomalous results due to diffusion of Alq_3 into the PDMS substrate. Conversely, a thin polystyrene (PS) film can be used as a diffusion barrier, enabling the elastic moduli to be accurately measured. Similar to most organic glasses, the Young's modulus of Alq_3 is on the order of 1 GPa and is statistically invariant for thicknesses >20 nm. Interestingly, there is a significant increase in the Young's modulus for thinner films. The modulus of a 10 nm Alq_3 film is found to be nearly twice that of a thicker film. Corresponding to this change in modulus is a loss of the optical adsorption peak associated with aggregation of Alq_3, which suggests that the modulus change is related to the local packing of the molecule. This result illustrates that the thickness of active layers in OLEDs impacts not only the device performance but also their elastic properties, both of which are important for use in flexible devices.

Introduction

Organic based electronics, in particular organic light emitting devices (OLEDs), have recently been incorporated into commercial flat panel displays,[1,2] but there is significant interest in extending these materials into cost effective *flexible* devices.[3–5] The potential fully organic electronic devices could be low-cost, lightweight, and compatible with the flexible substrates that are employed in well-established roll-to-roll printing techniques.[2,6] Tremendous efforts have been placed on developing additive processing on flexible substrates,[7–9] but relatively little attention has been paid to understanding their mechanics.[10,11] Traditional microelectronics utilizes strain in the silicon lattice to increase the semiconductor performance;[12] likewise the electrical and optical properties of organic materials could be strongly affected by their molecular packing, which could be easily influenced with different mechanical stresses imposed on the organic thin films.[13] Thus, how organic materials respond to strain during bending could be critical to the performance of flexible electronic devices.[14] The mechanics of flexible electronics utilizing inorganic

active components has been examined more rigorously due to their propensity for cracking, and a significant decrease in performance has been observed at strains much less than the strain at failure.[15] To begin to address this issue in the rapidly emerging field of organic electronics, the mechanical properties of organic electronic materials need to be understood at the corresponding scale associated with the actual devices.

There are numerous challenges involved in measuring the mechanical properties of organic electronic materials. First, many active materials are glassy films due to the commonly adopted vapor deposition or spin-casting method; thus, bulk measurements would likely not accurately capture the mechanical properties of the material in functioning devices. Furthermore, the expense of many OLED materials precludes the use of bulk tensile testing even if the bulk and thin film properties were identical. Nanoindentation (NI)[16] and Brillouin light scattering (BLS)[17] are commonly used to assess the elastic properties of films; however, for highly complaint materials like most organics and polymers, the mechanical properties of the substrate can be convoluted with those of the film of interest.[18] Application of atomic force microscopy (AFM) to control indentation depth has enabled the near surface modulus of glassy films to be determined. A reduced elastic modulus in the top (5 to 7) nm of polystyrene (PS) has been elucidated using this technique.[19] Conversely, Van Vliet and co-workers showed a significant increase in surface stiffness within 200 nm of the PS surface using nanoindentation.[20] Further, nanoindentation measurements of >100 nm thick films of a common OLED material, tris (8-hydroxyquinolinato)aluminium (Alq_3), have demonstrated a strong dependence of the elastic properties on the supporting

[a]Chemical Engineering, Arizona State University, Tempe, AZ, 85284, USA. E-mail: bryan.vogt@asu.edu
[b]Materials Engineering, Arizona State University, Tempe, AZ, 85284, USA
[c]Polymers Division, National Institute of Standards and Technology, Gaithersburg, MD, 20899, USA

† Electronic supplementary information (ESI) available: Ellipsometric data and fits, optical constants for additional films and micrograph of poorly wrinkled film. See DOI: 10.1039/c0sm00364f
‡ This paper is part of a *Soft Matter* themed issue on The Physics of Buckling. Guest editor: Alfred Crosby.

substrate.[10,11] On hard silicon substrates, the Alq_3 modulus is extrapolated to be on the order of 100 GPa; while on plastic substrates, the modulus of the same material is only on the order of 1 GPa.[10,11] One potential route to overcome these difficulties in determining the elastic modulus of soft materials in thin films is through the use of a surface wrinkling metrology, which employs an instability that occurs upon compression of a system consisting of a stiff film on a soft substrate.[21] This technique has been applied to determining the elastic moduli of ultrathin (down to 5 nm) polymer films[22,23] and organic electronic materials.[24] The latter study demonstrated that the mechanical properties of several active organic electronic materials could be determined using surface wrinkling for thicknesses (30 nm to 200 nm) comparable to those utilized in functional devices.[24]

The layers in many organic electronic devices, in particular OLEDs, are in the sub-50 nm range.[25] This length scale also corresponds with dimensions where the thermophysical behavior of glass forming materials has been shown to deviate from bulk properties.[22,23,26–29] Work on these confined systems reveal that either increased or decreased glass transition temperature (T_g) is dependent on the strength of the interaction between the wall of the pore and the confined liquid.[29–32] Not only is the T_g of small molecules impacted by confinement but so are the melting temperature,[33] crystallization,[29] and density.[33] The abundance of research into the thermal properties of confined organic glasses has been enhanced due to the availability of non-invasive measurement techniques.

Recently, we have investigated the mechanical properties of several confined polymer thin film systems.[22,23,34] For all glassy polymers examined, there is a decrease in the elastic modulus of ultrathin (<30 nm) films in comparison to the bulk modulus. The length scale at which deviations in the elastic moduli occur is found to scale with the bulk T_g of the polymer[23,35] in agreement with molecular simulations.[35] However, very little is known regarding the mechanical properties of organic molecular glasses at the nanoscale. Recently, Kearns et al. utilized BLS to determine the modulus of vapor deposited indomethacin films;[36] however, the films were required to be 10 μm to 15 μm thick.[36] Tahk et al. have utilized surface wrinkling to determine the elastic modulus of thin pentacene films prepared by vapor deposition.[24] These pentacene films are polycrystalline and have a reported elastic modulus of approximately 15 GPa. However; the quality of the wrinkles formed from the pentacene films is poor and apparent delamination occurs at modest strain (10%), thus we validate here the appropriateness of using surface wrinkling to elucidate the elastic properties of small molecule organic electronic materials.

In this article, the mechanical properties of sub-100 nm, vapor deposited Alq_3 films are determined using surface wrinkling. Alq_3 is widely used as an electron transporting layer and host material for various dyes in OLEDs due to its luminescent properties, high electron mobility, and high thermal and electrochemical stability.[37,38] Vapor deposited Alq_3 films are glassy and the modulus of >100 nm coatings have recently been estimated using NI.[10,11] However, the modulus is found to be strongly dependent upon the supporting substrate and the authors express uncertainty regarding the absolute value for the elastic modulus of Alq_3. In an attempt to mitigate substrate influences, the modulus of Alq_3 films ranging from 10 nm to 100 nm in thickness is determined using surface wrinkling. Not only does this provide the mechanical properties of Alq_3 that will enable a deeper understanding as to how bending/stretching will impact performance of OLEDs, these measurements provide the first experimental data demonstrating thickness-dependent moduli for an organic molecular glass.

Experimental

Note that certain commercial equipment, instruments, or materials are identified in this document. Such identification does not imply recommendation or endorsement by the National Institute of Standards and Technology (NIST), nor does it imply that the products identified are necessarily the best available for this purpose. The data throughout this paper are presented along with the standard uncertainty (±) involved with the measurement based on one standard deviation.

Alq_3 was purchased (Sigma Aldrich) and purified by repeated thermal evaporation. Polydimethylsiloxane (PDMS, Sylgard 184, Dow Corning) was prepared at a ratio of 20 : 1 or 10 : 1 by mass of base to curing agent and cast on float glass to a thickness of approximately 1.5 mm. The PDMS was allowed to react at ambient temperature for 3 h prior to curing at 100 °C for 2 h. After cooling to ambient temperature, the PDMS sheet was cut into approximately 75 mm × 25 mm × 1.5 mm slabs, which function as elastic substrates for the Alq_3 films. The modulus of the PDMS from each batch was determined using a Texture Analyzer (TA.XT Plus, Texture Technologies). Similarly, the optical constants for PDMS were determined from a Cauchy model to fit the ellipsometric angles determined using a Variable Angle Spectroscopic Ellipsometer (VASE, J. A. Woollam Co., Inc.) over a wavelength range from 250 nm to 1700 nm measured at three incident angles (67°, 70°, and 73°). The final preparation step for wrinkling was to pre-strain the PDMS to 3%.[39]

Alq_3 was deposited directly on the strained substrate using a resistively heated tantalum boat at pressures below 10^{-7} Torr in a vacuum thermal deposition system (Trovato Mfg.). A shadow mask restricted deposition to a 16 mm diameter circular pattern. Deposition rate was controlled between 1 Å s^{-1} and 1.5 Å s^{-1} with the use of crystal growth monitors. The film growth rate calibrations necessary to report absolute thin film thicknesses ranging from 8 nm to 100 nm were accomplished through agreement between three sources of measurement. First, direct measurements of the film(s) on PDMS were collected before and after small molecule deposition using VASE. Identical depositions for thicknesses representing the full range of experimental data were also performed with silicon substrates loaded in place of the PDMS, and their thickness was measured by both VASE and profilometry (P-6, KLA-Tencor). Profile scans were collected across shadow masked edges as well as ledges exposed by post-deposition removal of Kapton tape to enable sampling at the center of the film. All methods were in agreement, which confirm predictable deposition rates.

Initially, the structural stability of Alq_3 films on PDMS was monitored using spectroscopic ellipsometry and fit to a three-layer model consisting of a PDMS substrate, an intermixed layer, and a Cauchy layer representing Alq_3 (for wavelengths between 650 nm and 1700 nm). The intermixed layer was used to model the diffusion of Alq_3 into PDMS through weighting of the PDMS and Alq_3 optical constants.[40] Significant changes in the Alq_3 film thickness suggest that diffusion of Alq_3 into PDMS can obfuscate mechanical analyses.

To prevent diffusion of Alq$_3$ into the PDMS substrate, PS (molecular mass of 9.4 kg mol^{-1} and 492 kg mol^{-1}, Polymer Laboratories) was utilized as a diffusion barrier. PS films approximately 22 nm thick were spin cast onto ultraviolet/ozone (model 342, Jelight, Inc.) cleaned silicon wafers (450 μm thick) at 250 rad s^{-1} from dilute solution in toluene. To transfer the PS film to the PDMS, the polymer film supported on the silicon wafer was placed into contact with the strained PDMS. Once the film was softly bonded to the PDMS, the system was immersed in water. Due to differential adhesion in water, PS was transferred cleanly to the PDMS. Prior to Alq$_3$ deposition, the thickness of PS layer was determined using spectroscopic ellipsometry directly on the strained PDMS using a two-layer model (PDMS/PS). After deposition, the thickness of the Alq$_3$ layer was determined again using spectroscopic ellipsometry using a three-layer model (PDMS/PS/Alq$_3$). After thickness measurements were complete, the pre-strain on the PDMS was released at a rate of 0.1 mm s^{-1} at ambient temperature ($T = 21\,°C \pm 2\,°C$) in order to wrinkle the films.

Characterization of the wrinkled surface was performed using Atomic Force Microscopy (AFM, Park XE-150) in intermittent contact mode using a constant scan size of 10 μm × 10 μm, and optical microscopy (OM, Mititoyo Ultraplan FS-110) with an image resolution of 1024 pixels × 768 pixels. AFM images were analyzed using a 1D Fast Fourier Transform (FFT) in XEI software in order to obtain the wavelength of the wrinkles. Similarly, the wrinkling wavelength from the OM images was determined using a 1D FFT of the micrographs using custom written Matlab code.

Results and discussion

### Stability of Alq$_3$ films on PDMS

One of the first indications that Alq$_3$ films directly deposited onto PDMS are not stable is a change in the color of the as-deposited film over the course of several hours. To quantify the changes in the films, the ellipsometric angles, Ψ and Δ, for the film are obtained at 55° as a function of time. As shown in Fig. 1 when Alq$_3$ is deposited directly onto PDMS, there is a significant reduction in the film thickness as the film ages at ambient conditions. Although Alq$_3$ is known to be marginally unstable in air,[41] the change in thickness is too great to be attributed to degradation. PDMS formulated with 20 : 1 base to curing agent forms a network with a modulus of ~0.7 MPa. This loose network enables Alq$_3$ to diffuse into the PDMS substrate. After 150 min, the thickness of the Alq$_3$ layer decreased by 40%. By increasing the base to curing agent ratio to 10 : 1, the crosslink density of the PDMS increases leading to a modulus of ~2 MPa. Comparatively, Alq$_3$ deposited onto 10 : 1 PDMS exhibited a decrease in film thickness of 23% after 150 min, as shown in Fig. 1. It is interesting that the Alq$_3$ has sufficient mobility to diffuse into the PDMS as T_g for Alq$_3$ is approximately 130 °C. Attempts to wrinkle these films yield ill-defined structures. This result is reminiscent of the poorly formed wrinkles using pentacene vapor deposited onto PDMS reported by Tahk *et al.*[24] The low glass transition temperature of PDMS ($T_g = -125\,°C$)[42] and large free volume of PDMS appear to enable diffusion of Alq$_3$ and potentially other small molecules into the PDMS network;[43] this may lead to a poorly defined system for wrinkling analysis.
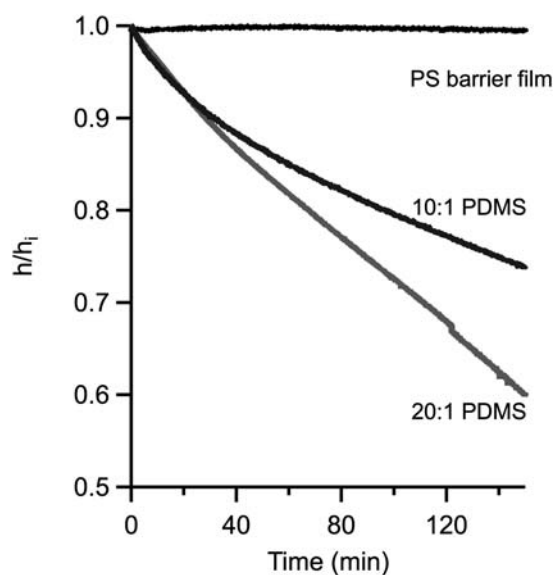
Fig. 1 Apparent Alq$_3$ normalized film thickness (h/h_i) as a function of time on 10 : 1 PDMS, 20 : 1 PMDS, and 20 : 1 PDMS with a 20 nm PS (9.4 kg mol^{-1}) barrier film. The decrease in thickness for the Alq$_3$ film for both bare PDMS substrates is attributed to diffusion of Alq$_3$ into the PDMS layer.

Thus, direct vapor deposition of small molecules on PDMS is likely problematic for determining their elastic moduli using wrinkling.

However, it is possible to prevent diffusion of Alq$_3$ into the PDMS substrate by addition of a barrier film; in this case, a nominal 20 nm PS film appears to prevent diffusion of the Alq$_3$ into the PDMS substrate, as shown in Fig. 1. The thickness of Alq$_3$ film remains invariant due to the limited free volume in PS and the slow glassy chain dynamics. This change in the diffusion behavior also has implications in the fabrication of organic devices on flexible plastic substrates as charge transport is defined by the interfacial morphology, which could be evolving as a result of diffusion of a glassy component. By insuring sharp interfaces with the use of a PS barrier film, the Alq$_3$/PS composite film on PDMS yields well defined wrinkles as illustrated in Fig. 2. An Alq$_3$ film ($h_{Alq_3} = 36$ nm) on a PS film ($h_{PS} = 22$ nm) wrinkles with a uniform wavelength of 3.5 μm ± 0.13 μm (Fig. 2a). Fig. 2b shows an AFM micrograph of an 8 nm Alq$_3$ film on 22 nm PS film with wavelength of 2.1 μm ± 0.15 μm. These well-defined wrinkles are similar to those observed for most glassy polymers, but the added PS layer must be included in the analysis of the wrinkling to deconvolute the elastic modulus of Alq$_3$.
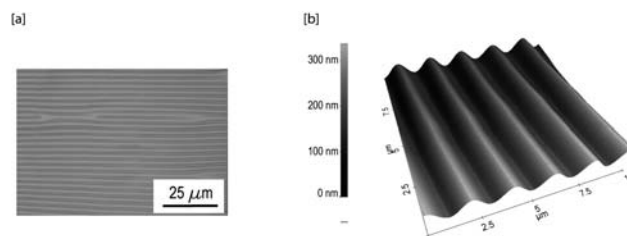
Fig. 2 [a] Optical image of a 36 nm Alq$_3$ film where the wavelength is 3.5 μm ± 0.13 μm. [b] AFM image of an 8 nm Alq$_3$ film with a 2.1 μm ± 0.15 μm wavelength.

Elastic modulus of Alq₃ films

The wrinkles in Fig. 2 are formed *via* uniaxial compression of the Alq₃/PS composite film on a PDMS substrate. The elastic properties of the composite system of PS and Alq₃ along with their thicknesses and elastic modulus of the PDMS dictate the wavelength of the wrinkle pattern. Thus, an effective plane-strain modulus of the Alq₃/PS composite film ($\bar{E}_{\text{eff}}$) can be determined from the wavelength, λ, by:

$$\bar{E}_{\text{eff}} = 3\bar{E}_{\text{s}}\left(\frac{\lambda}{2\pi d_{\text{t}}}\right)^3 \tag{1}$$

where d_{t} is the total thickness of the film, $h_{\text{PS}} + h_{\text{Alq}_3}$, and $\bar{E}_{\text{s}}$ is the plane-strain modulus of the PDMS. The mechanical contributions of each layer (PS and Alq₃) can be separated similar to previous derivations for two-plate composite films on PDMS.[39,44] In a similar manner, the modulus of Alq₃ can be calculated as:[44]

$$\bar{E}_{\text{Alq}_3} = \frac{\dfrac{\bar{E}_{\text{eff}}}{4} - \bar{E}_1\left[\left(\phi_{\text{ps}} - \dfrac{\kappa}{2}\right)^3 + \left(\dfrac{\kappa}{2}\right)^3\right]}{\left(1 - \dfrac{\kappa}{2}\right)^3 - \left(\phi_{\text{PS}} - \dfrac{\kappa}{2}\right)^3} \tag{2}$$

where $\kappa = \dfrac{1 + \phi_{\text{ps}}^2\left(\dfrac{\bar{E}_{\text{ps}}}{\bar{E}_{\text{Alq}_3}} - 1\right)}{1 + \phi_{\text{ps}}\left(\dfrac{\bar{E}_{\text{ps}}}{\bar{E}_{\text{Alq}_3}} - 1\right)}$ represents the deviation factor for

the neutral axis of bending, $\phi_{\text{ps}} = h_{\text{ps}}/(h_{\text{ps}} + h_{\text{Alq}_3})$ and ϕ_{ps} is the height fraction of PS. In order to calculate the modulus of the Alq₃ film, the Alq₃ and PS film thicknesses and the moduli of the PS film and the PDMS must be known. For these experiments, a constant PS film thickness of 21 nm ± 2 nm is used with a modulus of 3.61 GPa ± 0.26 GPa[34] and the modulus of the PDMS substrate varies between 0.6 MPa and 0.8 MPa depending upon the batch. With a single unknown, $\bar{E}_{\text{Alq}_3}$, eqn (2) is iteratively solved to determine the modulus of the Alq₃ film.

The Young's modulus, E_{Alq_3}, of the Alq₃ films can be determined from the plane-strain modulus, $\bar{E}_{\text{Alq}_3}$ as:

$$E_{\text{Alq}_3} = \bar{E}_{\text{Alq}_3}(1 - \nu^2_{\text{Alq}_3}) \tag{3}$$

where ν is the Poisson's ratio of the Alq₃. Recently, the Poisson's ratio of vapor deposited indomethacin (molecular glass) was determined to be 0.36 by BLS;[36] similarly, we have assumed $\nu = 0.33$ for the Alq₃ as this is the approximate Poisson's ratio for most organic glasses.[45] Based upon this assumption, the Young's modulus of the 36 nm thick Alq₃ film (Fig. 2a) is 0.94 GPa ± 0.18 GPa. This is significantly less than the estimated 100 GPa modulus for Alq₃ determined using 100 nm thick films on silicon wafers with NI.[10] The modulus obtained from NI is extremely large for an organic molecule and is similar to that of the hard support ($E_{\text{silicon}} = 130$ GPa). To assess if the difference in the modulus might be due to a surface chemistry effect that impacts the morphology, the optical constants for analogous films deposited on both PS/PDMS and silicon wafers have been determined using spectroscopic ellipsometry. There is no statistical difference in the optical constants for Alq₃ or surface morphology from AFM between films deposited on PS/PDMS or silicon wafers (see ESI†) and thus the substrate does not appear to be responsible for the large difference in modulus

between these measurements using wrinkling and prior NI results.[10] However, the modulus of most organic glass formers formed by supercooling the liquid is between 1 GPa and 2 GPa; these values are in agreement with the modulus of Alq₃ determined by wrinkling. Even for vapor deposited glasses, Kearns *et al.* have recently shown that the elastic modulus of indomethacin and trisnaphthylbenzene is between 4 GPa and 5 GPa using BLS.[36] It should be noted that the Young's modulus of these vapor deposited organic glasses is dependent on deposition conditions. Nonetheless, the elastic modulus of the Alq₃ film reported here appears to be reasonable based upon comparison to other organic molecular glasses.

For thin polymer films, a decrease in elastic modulus has generally been reported for thickness less than approximately 50 nm.[23,34,46] Thus, an even lower modulus for the 8 nm thick Alq₃ film might be expected if organic small molecules and polymers behave similarly at the nanoscale. However, the Young's modulus of the 8 nm thick Alq₃ film is calculated to be 1.66 GPa ± 0.21 GPa. This suggests that the modulus of Alq₃ increases if it is confined to nanoscale dimensions. Fig. 3 illustrates how the plane-strain modulus depends on film thickness. For films thicker than 20 nm, the modulus is independent of film thickness at approximately 1.0 GPa. This is similar to the modulus of pentacene, which has been shown to be independent of film thickness down to 25 nm.[24] However, as the film thickness of Alq₃ is reduced from 20 nm to 10 nm, the plane-strain modulus appears to increase significantly. For example, decreasing the thickness from 20 nm to 10 nm results in an increase in the plane-strain modulus from 1.01 GPa ± 0.27 GPa to 1.69 ± 0.32 GPa. Thus, there is nearly a 70% increase in the elastic properties of Alq₃ when confined to 10 nm. This large increase in elastic modulus is counter to most reports for glassy polymers where 10 nm films can exhibit a modulus that is 10% of the bulk.[22]
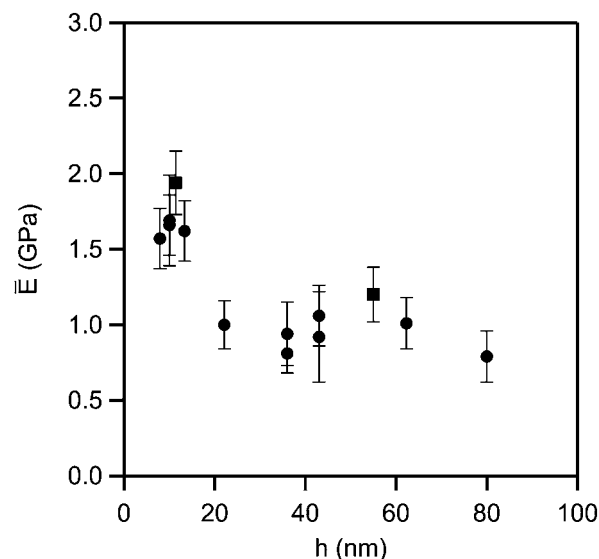

Fig. 3 Modulus as a function of film thickness for Alq₃ determined using (●) 9.4 kg mol⁻¹ PS and (■) 492 kg mol⁻¹ PS as diffusion barrier with the two-plate composite calculations. The error bars represent one standard deviation of the data, which is taken as the experimental uncertainty of the measurement.

One simple explanation for this increase could be interdiffusion of the Alq$_3$ partially into the PS film as the increased modulus is approaching that of PS. To assess this potential, two different molecular mass PS (below and above entanglement molecular mass) are used as barriers for the Alq$_3$ wrinkling experiments. As shown in Fig. 3, there is no difference in the calculated moduli for Alq$_3$ with the different barriers, but interdiffusion is typically much more prevalent in polymers below their entanglement molecular mass than above.[47] Thus, simple interdiffusion does not appear to be responsible for the observed increased moduli of Alq$_3$ for ultrathin films. However, enhancements in the yield strength and ductility of metallic glasses upon confinement to the nanoscale have been reported for a number of different systems.[48] Thus, enhancements in mechanical properties for Alq$_3$ upon confinement to the nanoscale are not completely unexpected. However, changes in the modulus for Alq$_3$ occur when the film is less than 20 nm thick, whereas enhancements in the yield stress of metallic glasses typically are observed at thicknesses greater than 100 nm.[48,49]

For polymeric materials, the decrease in elastic modulus for ultrathin films is attributed to a softening of the material near the free surface.[23] Therefore, it is plausible that changes in the structure of Alq$_3$ near interfaces could be responsible for the deviations in mechanical properties, especially considering the very small length scales at which changes in the elastic moduli are observed. By variation in the vapor deposition conditions, the Young's modulus of indomethacin and trisnaphthylbenzene films can be increased by 19% as a result of improved packing of the glass.[36] This change based upon deposition conditions is almost an order of magnitude less than the difference between thick and thin Alq$_3$ films determined here. However, vapor deposited pentacene shows a change in morphology as a function of thickness from a monolayer to more bulk-like dimensions.[50,51] The well ordered thin film structure transitions into a less ordered structure in the bulk during deposition,[50,51] but under optimal deposition conditions the well ordered structure persists up to thickness of 19 nm.[52] Interestingly, this critical thickness of 19 nm for the pentacene corresponds well to the thickness where a change in the modulus for Alq$_3$ is observed here. It is known that the change in morphology from thin film to bulk is accompanied by a corresponding change in the optical properties of the pentacene film. Thus, thickness dependent structure of the Alq$_3$ films should be marked by changes in the optical constant of the film as well.

To assess these changes, the absorption coefficient, k, is determined for each film using multiple angle spectroscopic ellipsometry. The optical constants for the Alq$_3$ film are determined by utilizing multiple Lorentzian oscillators to fit the ellipsometric angles following the procedure of Djurisic and co-workers.[53] Fig. 4 illustrates how the extinction coefficient varies with thickness for Alq$_3$ films ranging from 80 nm to 12 nm. For all films, there are two absorption peaks at 260 nm and 385 nm that correspond to those observed for a dilute Alq$_3$ solution.[54] These data suggest that these adsorption bands are associated with the isolated Alq$_3$ molecule. For the thicker films, another absorption band in the range of 310 nm to 340 nm is observed that is indicative of the formation of Alq$_3$ aggregates. The optical constants for the 80 nm Alq$_3$ film are consistent with those reported for a 150 nm thick Alq$_3$ film.[55] However, as the thickness of the film is reduced, the peak associated with dyads
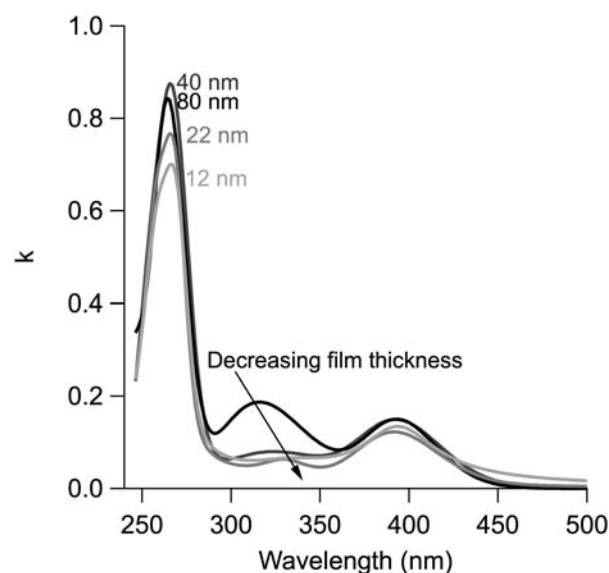
Fig. 4 Optical constant of Alq$_3$ films with thicknesses of 80 nm, 40 nm, 22 nm, and 12 nm. Peaks at 260 nm and 385 nm are present for all Alq$_3$ films with decreasing intensity as the film thickness is reduced. The intermediate adsorption band (310 nm to 340 nm) associated with aggregates of Alq$_3$ shifts to larger wavelength as the film thickness decreases with no peak observed for the 12 nm thick film.

(aggregates) shifts to higher wavelength, which suggests a change in the molecular packing. One additional change is a decrease in the molecular adsorption peaks at 260 nm and 385 nm. This decrease could be associated with interdiffusion of Alq$_3$ into the PS layer (diluting the adsorption as PS is transparent in this wavelength range) as porous Alq$_3$ films show a similar trend in decreased k.[56] However, these changes in the adsorption spectra also occur for thin films deposited on silicon wafers (see ESI†) and are thus not related to the interaction of the Alq$_3$ with the PS. Therefore, the changes in the adsorption spectra are likely related to the thin film morphology. A change in morphology would also be consistent with the observed variation in elastic modulus with thickness as shown in Fig. 3.

However, it is not well understood how different molecular packing influences the absorption energy and intensity. Moreover, the surface topography is nobular in all cases (see ESI†), although slightly rougher when deposited on PS. This is not unexpected as the PS/PDMS will initially be rougher than a silicon wafer. Thus, quantifying differences in the aggregates/morphology as a function of film thickness will require improved morphological characterization techniques and a more diverse group of materials to enable correlation of shifts in adsorption bands with aggregate size/shape. Future work will focus on attempting to correlate the changes of molecular packing with the modification of elastic modulus of different organic electronic materials.

It should be noted that previous studies on the modulus of thicker (100 nm) Alq$_3$ films on both poly(ethylene terephthalate) (PET) and silicon wafer substrates using NI are inconsistent with the current findings.[10] However, these moduli have shown significant substrate effects as the reported modulus of Alq$_3$ varies from ~13 GPa on PET to ~120 GPa on a silicon wafer;[10] these moduli are very similar to the modulus of the substrates themselves and suggest significant substrate interference. The wrinkling metrology

utilized here appears to be capable of mitigating these substrate effects, allowing accurate determination of the modulus of small organic glasses at the nanometre length scale.

Conclusion and outlook

In summary, the thin film modulus for Alq_3 was determined using surface wrinkling. Wrinkling of Alq_3 deposited directly on PDMS is significantly hindered and complicated by diffusion of Alq_3 into the PDMS substrate. A simple PS barrier film prevents diffusion of Alq_3 and allows the modulus to be determined with composite plate (or laminate) theory. The modulus of Alq_3 remains independent of thickness for films greater than 20 nm, while an increase in modulus is observed for thinner films. This increase in modulus is tentatively attributed to variations in molecule packing as a function of film thickness. The thin film optical constants determined from spectroscopic ellipsometry confirm a change in structure for the thin films.

Acknowledgements

References

1 Chem. Eng. News, 2007, **85**, 21–21.
2 S. R. Forrest, Nature, 2004, **428**, 911–918.
3 P. E. Burrows, V. Bulovic, Z. Shen, S. R. Forrest and M. E. Thompson, IEEE Trans. Electron Devices, 1997, **44**, 1188–1203.
4 T. W. Kelley, P. F. Baude, C. Gerlach, D. E. Ender, D. Muyres, M. A. Haase, D. E. Vogel and S. D. Theiss, Chem. Mater., 2004, **16**, 4413–4422.
5 M. D. McGehee, C. Goh, Frontiers of Engineering: Reports on Leading-Edge Engineering 2005 Symposium, 2006, pp. 119–130.
6 J. A. Rogers and Z. Bao, J. Polym. Sci., Part A: Polym. Chem., 2002, **40**, 3327–3334.
7 T. Kawase, H. Sirringhaus, R. H. Friend and T. Shimoda, Adv. Mater., 2001, **13**, 1601–1607.
8 R. Parashkov, E. Becker, T. Riedl, H. H. Johannes and W. Kowalsky, Proc. IEEE, 2005, **93**, 1321–1329.
9 H. Sirringhaus, T. Kawase, R. H. Friend, T. Shimoda, M. Inbasekaran, W. Wu and E. P. Woo, Science, 2000, **290**, 2123–2126.
10 C.-J. Chiang, S. Bull, C. Winscom and A. Monkman, Org. Electron., 2010, **11**, 450–455.
11 C.-J. Chiang, C. Winscom, S. Bull and A. Monkman, Org. Electron., 2009, **10**, 1268–1274.
12 M. L. Lee, E. A. Fitzgerald, M. T. Bulsara, M. T. Currie and A. Lochtefeld, J. Appl. Phys., 2005, **97**, 011101–011128.
13 J. E. Anthony, D. L. Eaton and S. R. Parkin, Org. Lett., 2002, **4**, 15–18.
14 R. J. Kline, D. M. DeLongchamp, D. A. Fischer, E. K. Lin, M. Heeney, I. McCulloch and M. F. Toney, Appl. Phys. Lett., 2007, **90**, 062117–062113.
15 H. Gleskova, I. C. Cheng, S. Wagner, J. C. Sturm and Z. Suo, Sol. Energy, 2006, **80**, 687–693.
16 G. M. Pharr and W. C. Oliver, MRS Bull., 1992, **17**, 28–33.
17 A. C. Ferrari, J. Robertson, M. G. Beghi, C. E. Bottani, R. Ferulano and R. Pastorelli, Appl. Phys. Lett., 1999, **75**, 1893–1895.
18 M. R. VanLandingham, J. S. Villarrubia, W. F. Guthrie and G. F. Meyers, Macromol. Symp., 2001, **167**, 15–43.
19 K. Miyake, N. Satomi and S. Sasaki, Appl. Phys. Lett., 2006, **89**, 031923–031925.
20 C. A. Tweedie, G. Constantinides, K. E. Lehman, D. J. Brill, G. S. Blackman and K. J. VanVliet, Adv. Mater., 2007, **19**, 2540–2546.
21 C. M. Stafford, C. Harrison, K. L. Beers, A. Karim, E. J. Amis, M. R. Vanlandingham, H. C. Kim, W. Volksen, R. D. Miller and E. E. Simonyi, Nat. Mater., 2004, **3**, 545–550.
22 C. M. Stafford, B. D. Vogt, C. Harrison, D. Julthongpiput and R. Huang, Macromolecules, 2006, **39**, 5095–5099.
23 J. M. Torres, C. M. Stafford and B. D. Vogt, ACS Nano, 2009, **3**, 2677.
24 D. Tahk, H. H. Lee and D.-Y. Khang, Macromolecules, 2009, **42**, 7079–7083.
25 Q. Qi, X. Wu, Y. Hua, Q. Hou, M. Dong, Z. Mao, B. Yin and S. Yin, Org. Electron., 2010, **11**, 503–507.
26 P. G. de Gennes, Eur. Phys. J. E: Soft Matter Biol. Phys., 2000, **2**, 201–203.
27 J. A. Forrest and K. Dalnoki-Veress, Adv. Colloid Interface Sci., 2001, **94**, 167–196.
28 J. A. Forrest and J. Mattsson, Phys. Rev. E: Stat. Phys., Plasmas, Fluids, Relat. Interdisc. Top., 2000, **61**, R53–R56.
29 C. L. Jackson and G. B. McKenna, J. Non-Cryst. Solids, 1991, **131**, 221–224.
30 P. Pissis, A. Kyritsis, D. Daoukaki, G. Barut, R. Pelster and G. Nimtz, J. Phys.: Condens. Matter, 1998, **10**, 6205–6227.
31 P. Scheidler, W. Kob and K. Binder, Europhys. Lett., 2002, **59**, 701–707.
32 J. Schuller, R. Richert and E. W. Fischer, Phys. Rev. B: Condens. Matter Mater. Phys., 1995, **52**, 15232–15238.
33 C. L. Jackson and G. B. McKenna, J. Chem. Phys., 1990, **93**, 9002–9011.
34 J. M. Torres, C. M. Stafford and B. D. Vogt, Polymer, article in press, DOI: 10.1016/j.polymer.2010.07.003.
35 K. Yoshimoto, T. S. Jain, P. F. Nealey and J. J. de Pablo, J. Chem. Phys., 2005, **122**, 144712.
36 K. L. Kearns, T. Still, G. Fytas and M. D. Ediger, Adv. Mater., **22**, 39–42.
37 J. R. Lian, Y. B. Yuan, L. F. Cao, J. Zhang, H. Q. Pang, Y. F. Zhou and X. Zhou, J. Lumin., 2010, **122–123**, 660–662.
38 C. W. Tang and S. A. VanSlyke, Appl. Phys. Lett., 1987, **51**, 913.
39 C. M. Stafford, S. Guo, C. Harrison and M. Y. M. Chiang, Rev. Sci. Instrum., 2005, **76**, 062207–062213.
40 C. M. Herzinger, B. Johs, W. A. McGahan, J. A. Woollam and W. Paulson, J. Appl. Phys., 1998, **83**, 3323.
41 P. Vivo, J. Jukola, M. Ojala, V. Chukharev and H. Lemmetyinen, Sol. Energy Mater. Sol. Cells, 2008, **92**, 1416–1420.
42 J. C. Lotters, W. Olthuis, P. H. Veltink and P. Bergveld, J. Micromech. Microeng., 1997, **7**, 145–147.
43 R. Gobel, R. Krska, R. Kellner, R. W. Seitz and S. A. Tomellini, Appl. Spectrosc., 1994, **48**, 678–683.
44 A. J. Nolte, R. E. Cohen and M. F. Rubner, Macromolecules, 2006, **39**, 4841–4847.
45 S. S. Jiping Ye, S. Sato, N. Kojima and J. Noro, MRS Bull., 2006, **F11**, 0914.
46 J. H. Zhao, M. Kiene, C. Hu and P. S. Ho, Appl. Phys.Lett., 2000, **77**, 2843–2845.
47 E. Jabbari and N. A. Peppas, J. Mater. Sci., 1994, **29**, 3969–3978.
48 D. C. Jang and J. R. Greer, Nat. Mater., 2010, **9**, 215–219.
49 C. A. Volkert, A. Donohue and F. Spaepen, J. Appl. Phys., 2008, **103**, 083539–083545.
50 I. P. M. Bouchoms, W. A. Schoonveld, J. Vrijmoeth and T. M. Klapwijk, Synth. Met., 1999, **104**, 175–178.
51 S. E. Fritz, S. M. Martin, C. D. Frisbie, M. D. Ward and M. F. Toney, J. Am. Chem. Soc., 2004, **126**, 4084–4085.
52 R. Ruiz, A. C. Mayer, G. G. Malliaras, B. Nickel, G. Scoles, A. Kazimirov, H. Kim, R. L. Headrick and Z. Islam, Appl. Phys. Lett., 2004, **85**, 4926–4928.
53 A. B. Djurisic, C. Y. Kwong, W. L. Guo, T. W. Lau, E. H. Li, Z. T. Liu, H. S. Kwok, L. S. M. Lam and W. K. Chan, Thin Solid Films, 2002, **416**, 233–241.
54 A. Aziz and K. L. Narasimhan, Synth. Met., 2000, **114**, 133–137.
55 C. Himcinschi, N. Meyer, S. Hartmann, M. Gersdorff, M. Friedrich, H. H. Johannes, W. Kowalsky, M. Schwambera, G. Strauch, M. Heuken and D. R. T. Zahn, Appl. Phys. A: Mater. Sci. Process., 2005, **80**, 551–555.
56 C. Himcinschi, O. Gordan, G. Salvan, F. Muller, D. R. T. Zahn, C. Cobet, N. Esser and W. Braun, Appl. Phys. Lett., 2005, **86**, 111907.